Proceedings of the
International Conference on Mechanical Engineering 2011
(ICME2011) 18-20 December 2011, Dhaka, Bangladesh

ICME11-FL-011

FINITE DIFFERENCE SOLUTION OF MHD RADIATIVE BOUNDARY LAYER FLOW OF A NANOFLUID PAST A STRETCHING SHEET

Md. Shakhaoath Khan[1], Md. Mahmud Alam[1] and M. Ferdows[2]

[1]Mathematics Discipline, Khulna University, Khulna-9208, Bangladesh
[2]Departments of Mathematics, University of Dhaka, Dhaka-1000, Bangladesh

ABSTRACT

Unsteady heat and mass flow of a nanofluid past a stretching sheet with thermal radiation in the presence of magnetic field is studied. To obtain non-similar equation, continuity, momentum, energy and concentration equations have been non-dimensionalised by usual transformation. The non-similar solutions are presented here which depends on the Magnetic parameter M , Radiation parameter R , Prandtl number P_r , Eckert number E_c , Lewis number L_e , Brownian motion parameter N_b and Thermophoresis parameter N_t respectively . The obtained equations have been solved by explicit finite difference method. The temperature and concentration profiles are discussed for the different values of the above parameters with different time steps.

Keywords: Nanofluid, Magnetic Field, Radiation, Stretching Sheet.

1. INTRODUCTION

The effect of thermal radiation on Magnetohydrodynamics (MHD) boundary layer flow has become important in several industrial, scientific and engineering fields. Due to sundry application of MHD as the design of heat exchangers, pumps and flow matters, in space vehicle propulsion, thermal protection, controlling the rate of cooling, controlling fusion etc, it's become more important for the flow due to a stretching surface. This study finds application in industries such as melt spinning, extrusion, glass fiber production, the hot rolling, wire drawing, manufacture of plastic and rubber sheets, polymer sheet and filaments etc. It's employed for copper, brass, bronze and aluminum and increasingly with cast iron and steel also.

Wang **[1]** investigate the problem of three dimensional fluid flows due to a stretching flat plate. Na and Pop **[2]** studied an unsteady flow past a stretching sheet. In the case of unsteady boundary layer flow, Sattar and Alam **[3]** presented unsteady free convection and mass transfer flow of a viscous, incompressible and electrically conducting fluid past a moving infinite vertical porous plate with thermal diffusion effect.

Jangid and Tomer **[4]** studied the effect of thermal radiation and magnetic field on unsteady stretching permeable sheet in presence of free stream velocity.

The technologies due to nanoparticles have been used over a large area. Choi **[5]** was the first author who studied nanoparticles. The analysis of convective instability and heat transfer characteristics of the nanofluids was investigated by Kang and Choi **[6]**.

Recently; Khan and Pop **[7]** have showed the problem of laminar boundary layer flow of a nanofluid past a stretching sheet. The natural Convective Boundary layer Flow of a nanofluid past a Vertical Plate have studied by Kuznestov and Neild **[8]**. In this model Brownian motion and Thermophoresis are accounted with the simplest possible boundary conditions.

Hence our aim is to study unsteady boundary layer nanofluid flow over a stretching surface with the influence of magnetic and thermal radiation effect. Explicit finite difference method **[9]** has been used to solve the obtained non- similar equations.

2. MATHEMATICAL MODEL OF FLOW

Considered the Cartesian coordinates x , measured along the stretching surface and y is the coordinate measured normal to the stretching surface. The physical configuration and coordinate system are shown in Fig 1. The flow takes place at $y \geq 0$. An unsteady uniform stress leading to equal and opposite forces is applied along the X-axis, so that the sheet is stretched keeping the origin fixed.

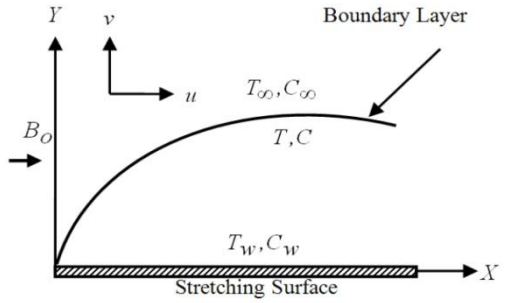

Fig 1. Physical model and coordinates system.

Initially it is assumed that fluid and the plate are at rest after that the plate is moved with a constant velocity U_0 in its own plane. Instantaneously at time $t > 0$, temperature of the plate and species concentration are raised to $T_w\left(>T_\infty\right)$ and $C_w\left(>C_\infty\right)$ respectively, which are thereafter maintained constant, where T_w, C_w are temperature and species concentration at the wall and T_∞, C_∞ are temperature and species concentration far away from the plate respectively. A uniform magnetic field B_0 is imposed to the plate. The magnetic induction vector B_0 can be taken as $B=\left(0,B_0,0\right)$. And q_r is radiative heat flux in the y-direction. Under the usual boundary layer approximation, the MHD unsteady nanofluid flow and heat and mass transfer with the radiation effect are governed by the following equations.

The Continuity equation,

$$\frac{\partial u}{\partial x}+\frac{\partial v}{\partial y}=0 \tag{1}$$

The Momentum equation,

$$\frac{\partial u}{\partial t}+u\frac{\partial u}{\partial x}+v\frac{\partial u}{\partial y}=U\frac{dU}{dx}+\upsilon\frac{\partial^2 u}{\partial y^2}+\frac{\sigma {B_0}^2}{\rho}(U-u) \tag{2}$$

The Energy equation

$$\frac{\partial T}{\partial t}+u\frac{\partial T}{\partial x}+v\frac{\partial T}{\partial y}=\alpha\frac{\partial^2 T}{\partial y^2}-\frac{\alpha}{k}\frac{\partial q_r}{\partial y}+\frac{\upsilon}{c_p}\left(\frac{\partial u}{\partial y}\right)^2 +\tau\left\{D_B\left(\frac{\partial T}{\partial y}\cdot\frac{\partial C}{\partial y}\right)+\frac{D_T}{T_\infty}\left(\frac{\partial T}{\partial y}\right)^2\right\} \tag{3}$$

The Concentration equation

$$\frac{\partial C}{\partial t}+u\frac{\partial C}{\partial x}+v\frac{\partial C}{\partial y}=D_B\frac{\partial^2 C}{\partial y^2}+\frac{D_T}{T_\infty}\frac{\partial^2 T}{\partial y^2} \tag{4}$$

the initial and boundary conditions are

$$\begin{aligned} &t=0,\ u_w=U_0=ax,\ v=0, T=T_\infty,\ C=C_\infty \quad \text{everywhere}\\ &t\geq 0,\ u=0,\ v=0,\ T=T_\infty,\ C=C_\infty \quad \text{at } x=0\\ &\quad u=U=bx,\ v=0,\ T=T_w,\ C=C_w \quad \text{at } y=0\\ &\quad u=0,\ v=0,\ T\to T_\infty,\ C\to C_\infty \quad \text{as } y\to\infty \end{aligned} \tag{5}$$

where α is the thermal diffusivity, k is the thermal conductivity, D_B is the brownian diffusion coefficient, D_T is the thermophoresis diffusion coefficient, where, X is the coordinate measured along stretching surface, u_w is the stretching velocity, U is the uniform velocity.

The Rosseland approximation **[10]** is expressed for radiative heat flux and leads to the form as,

$$q_r=-\frac{4\sigma}{3\kappa^*}\frac{\partial T^4}{\partial y} \tag{6}$$

where σ is the Stefan-Boltzmann constant and κ^* is the mean absorption coefficient. The temperature difference with in the flow is sufficiently small such that T^4 may be expressed as a linear function of the temperature, then the Taylor's series for T^4 about T_∞ after neglecting higher order terms,

$$T^4=4T_\infty{}^3-3T_\infty{}^4 \tag{7}$$

Introducing the following non dimensional variables, the equation (1) to (5) become,

$$X=\frac{xU_0}{\upsilon},\quad Y=\frac{yU_0}{\upsilon},\quad U=\frac{u}{U_0},\quad V=\frac{v}{U_0},\quad \tau=\frac{tU_0^2}{\upsilon},\quad \bar{T}=\frac{T-T_\infty}{T_w-T_\infty},\quad \bar{C}=\frac{C-C_\infty}{C_w-C_\infty}.$$

$$\frac{\partial U}{\partial X}+\frac{\partial V}{\partial Y}=0 \tag{8}$$

$$\frac{\partial U}{\partial \tau}+U\frac{\partial U}{\partial X}+V\frac{\partial U}{\partial Y}=\frac{1}{Re}\left(\frac{b^2}{a^2}\right)+\frac{\partial^2 U}{\partial Y^2}+M(1-U) \tag{9}$$

$$\frac{\partial \bar{T}}{\partial \tau}+U\frac{\partial \bar{T}}{\partial X}+V\frac{\partial \bar{T}}{\partial Y}=\left(\frac{1+R}{P_r}\right)\frac{\partial^2 \bar{T}}{\partial Y^2}+E_c\left(\frac{\partial U}{\partial Y}\right)^2 +N_b\left(\frac{\partial \bar{T}}{\partial Y}\cdot\frac{\partial \bar{C}}{\partial Y}\right)+N_t\left(\frac{\partial \bar{T}}{\partial Y}\right)^2 \tag{10}$$

$$\frac{\partial \bar{C}}{\partial \tau}+U\frac{\partial \bar{C}}{\partial X}+V\frac{\partial \bar{C}}{\partial Y}=\frac{1}{L_e}\left[\frac{\partial^2 \bar{C}}{\partial Y^2}+\left(\frac{N_t}{N_b}\right)\frac{\partial^2 \bar{T}}{\partial Y^2}\right] \tag{11}$$

the non-dimensional boundary conditions are;

$$\tau\leq 0,\ U=0,\ V=0,\ \bar{T}=0,\ \bar{C}=0 \quad \text{everywhere} \tag{12}$$

$$\begin{aligned} &\tau>0,\ U=0,\ V=0,\ \bar{T}=0,\ \bar{C}=0 \quad \text{at } X=0\\ &\quad U=1,\ V=0,\ \bar{T}=1,\ \bar{C}=1 \quad \text{at } Y=0\\ &\quad U=0,\ V=0,\ \bar{T}=0,\ \bar{C}=0 \quad \text{as } Y\to\infty \end{aligned} \tag{13}$$

where, Magnetic parameter $M=\frac{\sigma {B_0}^2\nu}{\rho U_0^2}$, Radiation parameter $R=\frac{16\sigma T_\infty{}^3}{3k\kappa^*}$, Prandtl number $P_r=\frac{\upsilon}{\alpha}$, Eckert number $E_c=\frac{{U_0}^2}{c_p(T_w-T_\infty)}$, Lewis number $L_e=\frac{\upsilon}{D_B}$, Brownian parameter $N_b=\frac{\tau D_B\left(C_w-C_\infty\right)}{\upsilon}$, Thermophoresis parameter $N_t=\frac{D_T}{T_\infty}\frac{\tau}{\nu}\left(T_w-T_\infty\right)$ and local Reynolds number $Re=\frac{xu_w}{\upsilon}$.

3. NUMERICAL PROCEDURE

In order to solve the non-similar unsteady coupled non-linear partial differential equations, the explicit

finite difference method has been used.

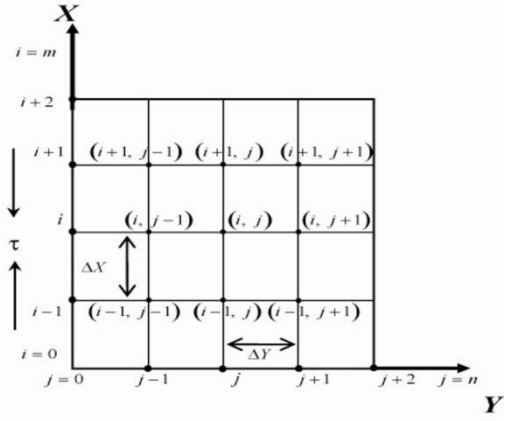

Fig 2**.** Finite difference space grid.

For this, a rectangular region of the flow field is chosen and the region is divided into a grid of lines parallel to *X* and *Y* axes, where *X*-axis is taken along the plate and *Y*-axis is normal to the plate. Here the plate of height $X_{\max}(=100)$ is considered i.e. *X* varies from 0 to 100 and assumed $Y_{\max}(=25)$ as corresponding to $Y \to \infty$ i.e. *Y* varies from 0 to 25. There are $m(=125)$ and $n(=125)$ grid spacing in the *X* and *Y* directions respectively as shown in Fig 2**.** It is assumed that ΔX , ΔY are constant mesh sizes along *X* and *Y* directions respectively and taken as follows,

$\Delta X = 0.8(0 \le X \le 100)$ and $\Delta Y = 0.2(0 \le Y \le 25)$

with the smaller time-step, $\Delta\tau = 0.005$.

Let U', V', $\bar{T}'$ and $\bar{C}'$ denote the values of U , V , $\bar{T}$ and $\bar{C}$ at the end of a time-step respectively. Using the explicit finite difference approximation, the following appropriate set of finite difference equations are obtained as;

$$\frac{U'_{i,j} - U'_{i-1,j}}{\Delta X} + \frac{V_{i,j} - V_{i,j-1}}{\Delta Y} = 0 \qquad (14)$$

$$\frac{U'_{i,j} - U_{i,j}}{\Delta\tau} + U_{i,j}\frac{U_{i,j} - U_{i-1,j}}{\Delta X} + V_{i,j}\frac{U_{i,j+1} - U_{i,j}}{\Delta Y} = \frac{1}{Re}\left(\frac{b^2}{a^2}\right) + \frac{U_{i,j+1} - 2U_{i,j} + U_{i,j-1}}{(\Delta Y)^2} + M\left(1 - U_{i,j}\right) \qquad (15)$$

$$\frac{\bar{T}'_{i,j} - \bar{T}_{i,j}}{\Delta\tau} + U_{i,j}\frac{\bar{T}_{i,j} - \bar{T}_{i-1,j}}{\Delta X} + V_{i,j}\frac{\bar{T}_{i,j+1} - \bar{T}_{i,j}}{\Delta Y} = \left(\frac{1+R}{P_r}\right)\left(\frac{\bar{T}_{i,j+1} - 2\bar{T}_{i,j} + \bar{T}_{i,j-1}}{(\Delta Y)^2}\right) + E_c\left(\frac{U_{i,j+1} - U_{i,j}}{\Delta Y}\right)^2 + N_b\left(\frac{\bar{T}_{i,j+1} - \bar{T}_{i,j}}{\Delta Y}\cdot\frac{\bar{C}_{i,j+1} - \bar{C}_{i,j}}{\Delta Y}\right) + N_t\left(\frac{\bar{T}_{i,j+1} - \bar{T}_{i,j}}{\Delta Y}\right)^2 \qquad (16)$$

$$\frac{\bar{C}'_{i,j} - \bar{C}_{i,j}}{\Delta\tau} + U_{i,j}\frac{\bar{C}_{i,j} - \bar{C}_{i-1,j}}{\Delta X} + V_{i,j}\frac{\bar{C}_{i,j+1} - \bar{C}_{i,j}}{\Delta Y} = \frac{1}{L_e}\left[\left(\frac{\bar{C}_{i,j+1} - 2\bar{C}_{i,j} + \bar{C}_{i,j-1}}{(\Delta Y)^2}\right) + \frac{N_t}{N_b}\left(\frac{\bar{T}_{i,j+1} - 2\bar{T}_{i,j} + \bar{T}_{i,j-1}}{(\Delta Y)^2}\right)\right] \qquad (17)$$

with initial and boundary conditions

$$U^0_{i,j} = 0,\ V^0_{i,j} = 0,\ \bar{T}^0_{i,j} = 0,\ \bar{C}^0_{i,j} = 0 \qquad (18)$$

$$U^n_{0,j} = 0,\ V^n_{0,j} = 0,\ \bar{T}^0_{0,j} = 0,\ \bar{C}^n_{0,j} = 0$$
$$U^n_{i,0} = 1,\ V^n_{i,0} = 0,\ \bar{T}^n_{i,0} = 1,\ \bar{C}^n_{i,0} = 1 \qquad (19)$$
$$U^n_{i,L} = 0,\ V^n_{i,L} = 0,\ \bar{T}^n_{i,L} = 0,\ \bar{C}^n_{i,L} = 0, \text{ where } L \to \infty$$

Here the subscripts i and j designate the grid points with X and Y coordinates respectively and the superscript n represents a value of time, $\tau = n\cdot\Delta\tau$ where $n = 0, 1, 2, \ldots$. Stability conditions and the convergence criteria are not shown for brevity.

4. RESULTS AND DISCUSSION

In order to investigate the physical representation of the problem, the numerical values of temperature and species concentration within the boundary layer have been computed for different values of Magnetic parameter M , Radiation parameter R , Prandtl number Pr , Reynolds number Re , Eckert number E_c , Lewis number Le , Brownian motion parameter N_b and Thermophoresis parameter N_t . To obtain the steady-state solutions of the computation, the calculation have been carried out up to non-dimensional time, $\tau = 5 \text{ to } 80$. The temperature and concentration profiles doesn't show any change after non-dimensional time, $\tau = 40$. Therefore the solution for $\tau \ge 40$ is steady-state solution. The graphical representations of the problem are showed in Comparison Figs 4, 6,8,10 and Figs 11-16. And these results have been compared with the published results of Khan and Pop **[7]** (see comparison figs 3, 5, 7, 9).

Comparison Fig 3. shows the effects of Brownian parameter Nb and thermophoresis parameter Nt on the temperature profile for Prandtl number $Pr = 10$, Lewis number $Le = 10$. For comparison with Fig 4, the values of radiation parameter R , magnetic parameter M , Eckert number E_c , stretching constant value $\frac{b}{a}$ are considered zero. Then it is observed that, temperature increases as the thermophoresis parameter Nt and the Brownian motion parameter Nb increases. Therefore qualitative agreement has been seen in these figures but not quantitative.

Comparison Fig 5. represents the concentration distribution for the different values of Nb and $Pr = 10$, $Le = 10$, $Nt = 0.1$, For comparison with Fig 6, the values of radiation parameter R , magnetic parameter M , Eckert number E_c , stretching constant value $\frac{b}{a}$ are considered zero. Here the thickness of the boundary layer for the mass fraction function is found to be smaller than the thermal boundary layer thickness when $Le > 1$. The concentration profiles are decreases with increase in Brownian parameter Nb . Therefore qualitative agreement has been seen in these figures but not quantitative.

Comparison Fig 7. represents the effects of Pr and Le on the temperature distribution for $Nb = 0.5$, and $\mathrm{Nt} = 0.5$. For comparison with Fig 8, the values of radiation parameter R, magnetic parameter M , Eckert number E_c ,

stretching constant value $\frac{b}{a}$ are considered zero. The temperature profiles increases with increasing in both Prandtl number Pr and Lewis number Le. Therefore qualitative agreement has been seen in these figures but not quantitative.

Comparison Fig 9. represents the effects of Le on the concentration profiles for $Pr = 10$, $Nt = 0.1$ and $Nb = 0.1$. For comparison with Fig 10, the values of radiation parameter R, magnetic parameter M, Eckert number E_c, stretching constant value $\frac{b}{a}$ are considered zero. When Le is increases, the concentration profiles decreases for several parameters. Therefore qualitative agreement has been seen in these figures but not quantitative.

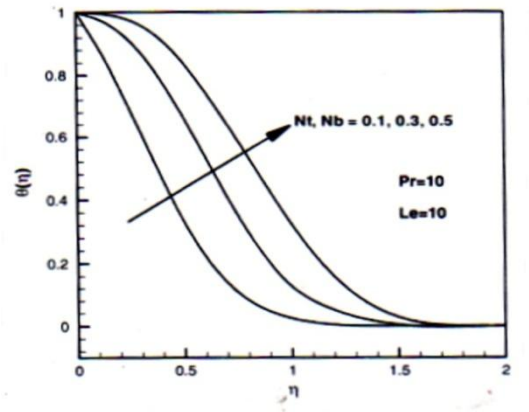

Comparison Fig 3. Effect of Nb and Nt on temperature profiles for specified parameters. (Similar problem)

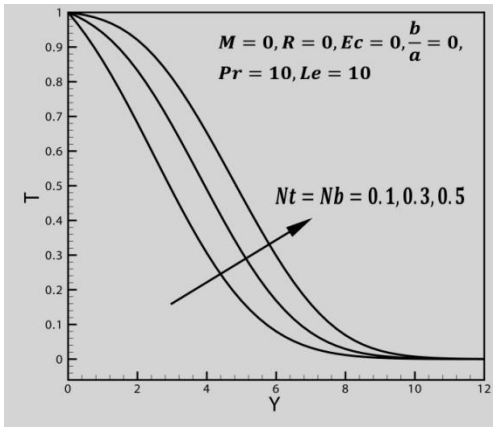

Comparison Fig 4. Steady-state ($\tau = 40$ and $\Delta\tau = 0.005$) temperature profiles for different values of Nb and Nt. (Non-similar problem)

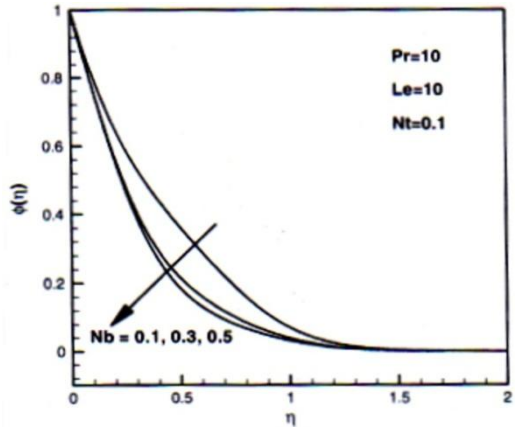

Comparison Fig 5. Effect of Nb on concentration profiles for specified parameters. (Similar problem)

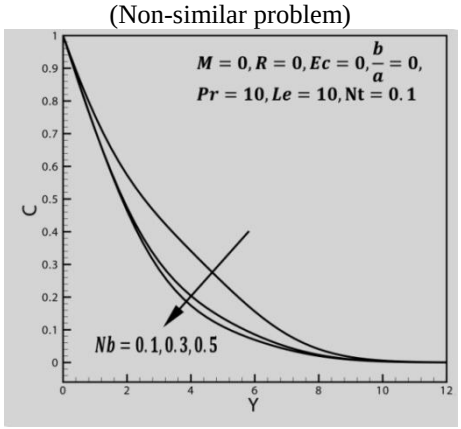

Comparison Fig 6. Steady-state ($\tau = 40$ and $\Delta\tau = 0.005$) concentration profiles for different values of Nb. (Non-similar problem)

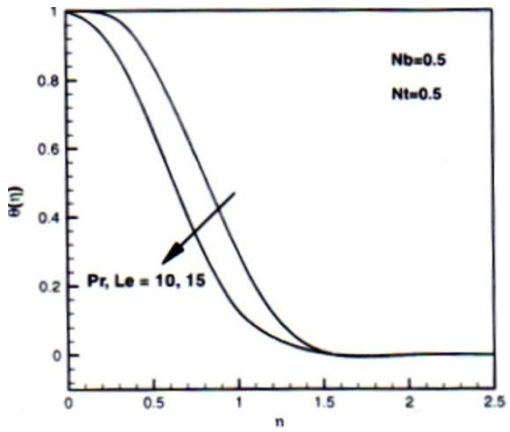

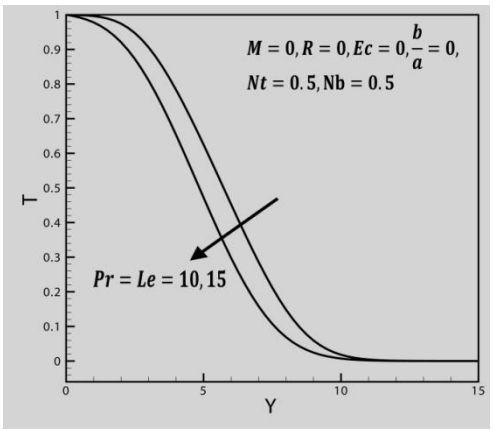

Comparison Fig7. Effect of Pr and Le on temperature profiles for specified parameters. (Similar problem)

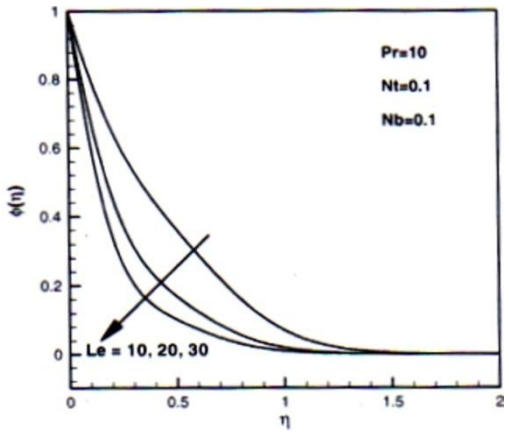

Comparison Fig 9. Effect of Le on concentration Profiles for specified parameters. (Similar problem)

Comparison Fig 8. Steady-state ($\tau = 40$ and $\Delta\tau = 0.005$) temperature profiles for different values of Pr and Le. (Non-similar problem)

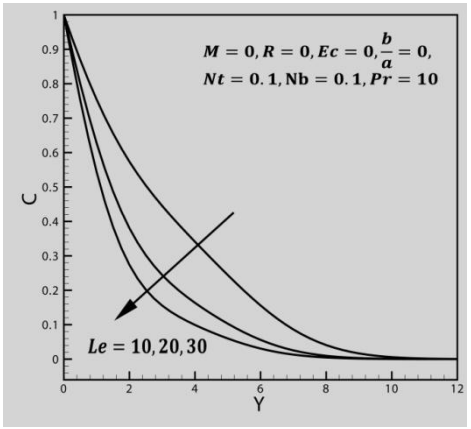

Comparison Fig10.Steady-state $(\tau = 40$ and $\Delta\tau = 0.005)$ Concentration profiles for different values of Le. (Non-similar problem)

In Figs. 11–16 the dimensionless temperature and concentration distributions are plotted against Y respectively for the different time step and different values of parameters. In Figs. 11 and 12 the temperature and concentration profiles are plotted respectively for different values of Nb. Here concentration profiles are decreases with increase of Nb, while the reverse effects have been obtained for temperature profile.

Dimensionless temperature distribution showed for different values of Prandtl number Pr in Fig. 13. As Pr increases, the temperature decreases. And Fig. 14 shows the dimensionless concentration distribution for different values of Le. Here the concentration profiles are decreases with increase in Le.

Figs. 15 and 16 show temperature gradually increases whereas the concentration decreases for increasing of R,

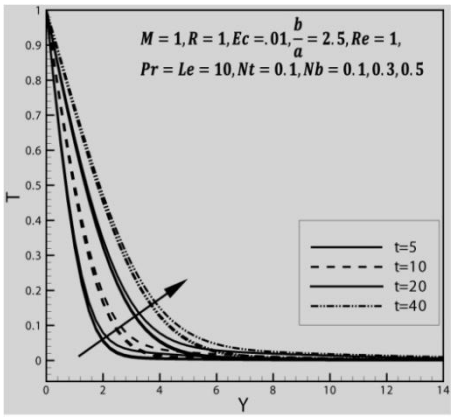

Fig 11. Temperature profiles for different values of *Nb* .

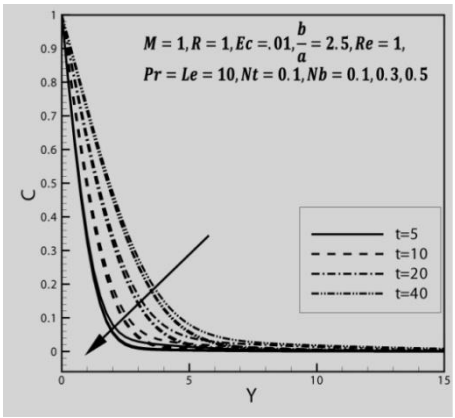

Fig 12. Concentration profiles for different values of *Nb* .

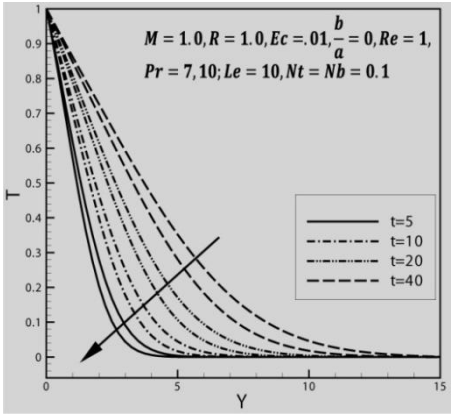

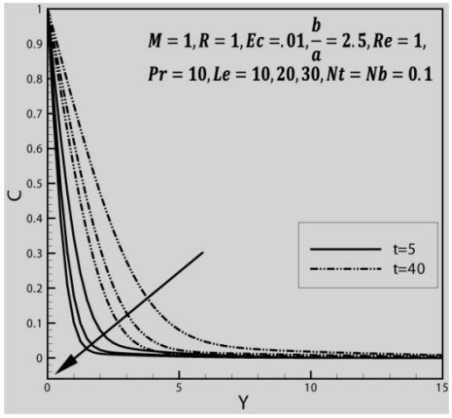

Fig 13. Temperature profiles for different values of $\Pr$.

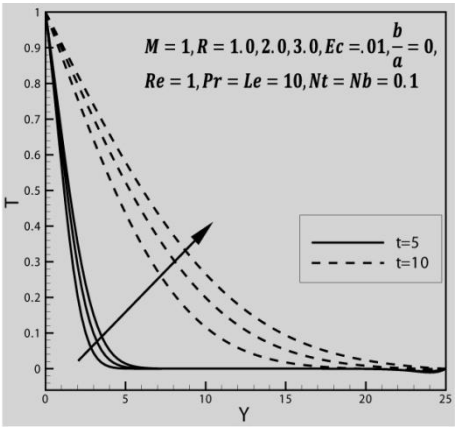

Fig 14. Concentration profiles for different values of Le.

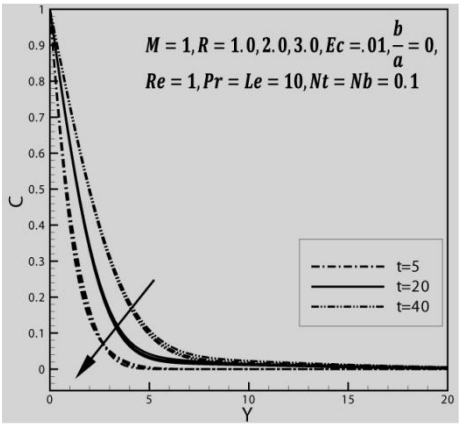

Fig 15. Temperature profiles for different values of R.

Fig 16. Concentration profiles for different values of R.

5. CONCLUSIONS

1. For increasing the Brownian and Thermophoresis parameter, temperature profiles increases whereas the concentration profiles decreases for increasing the Brownian parameter.
2. Thermal boundary layer thickness decreases for increasing Prandtl number and concentration boundary layer thickness decreases for increasing Lewis number.
3. The MHD and Radiation effect through the boundary layer for both temperature and concentration has a great impact on flow pattern. As the radiation parameter increases then the temperature gradually increases while the reverse effects seen for concentration profiles.
4. A considerable comparison with Khan and Pop **[7]** has been showed.

6. REFERENCES

1. Wang, C.Y., 1984, "The three-dimensional flow due to a stretching surface", *Physics of Fluids* 27, pp. 1915-1917.
2. Na T.Y. and Pop I., 1996, "Unsteady flow past a stretching sheet", *Mechanics Research Communications*, vol.23, pp. 413-422.
3. Sattar, M.A. and Alam, M.M., 1994, "Thermal Diffusion as well as transpiration effects on MHD free convection and mass transfer flow past an accelerated vertical porous plate", *Indian Journal of pure applied Mathematics*, 25(6), pp. 679-688.
4. Singh. P., Jangid, Tomer.N.S. and Sinha. D., 2010, "Effects of Thermal Radiation and Magnetic Field on Unsteady Stretching Permeable Sheet in Presence of Free Stream Velocity", *International Journal of Information and Mathematical Science*, 6:3.
5. Choi,S.U.S., 1995, "Enhancing thermal conductivity of fluids with nanoparticles", in: *The proceedings of the 1995 ASME International Mechanical Engineering Congress and Exposition*, San Fransisco, USA, ASME, FED 231/MD 66, pp. 99-105.
6. Kang, Ki, J., Y. T., and Choi, C. K., 2004, "Analysis of Convective Instability and Heat Transfer Characteristics of Nanofluids", *Physics of Fluids*, 16 (7), pp. 2395-2401.
7. Khan, W.A. and Pop, I., 2010, "Boundary-Layer Flow of a Nanofluid Past a Stretching Sheet", *International Journal of Heat and Mass Transfer*, Vol. 53, pp. 2477-2483.
8. Kuznetsov, A.V. and Nield, D.A., 2010 "Natural Convective Boundary- layer Flow of a Nanofluid Past a Vertical Plate", *International Journal of Thermal Sciences*, Vol. 49, pp. 243 -247.
9. Carnahan B., Luther H.A. and Wilkes J.O., 1969 "*Applied Numerical Methods*", John Wiley and sons, New York.
10. Rohsenow, W.M., J.P. Harnett and Y.I. Cho., 1998 "*Handbook of Heat transfer*", 3rd edition, McGraw-Hill, New York.

7. NOMENCLATURE

Symbol	Meaning	Unit
u, v	Velocity components	(ms^{-1})
υ	Kinematic viscosity	(m^2s^{-1})
ρ	Density of fluid	(kgm^{-3})
τ	Dimensionless time	
U, V	Dimensionless velocity components	
$\bar{T}$	Dimensionless temperature	
$\bar{C}$	Dimensionless concentration	
q_r	Radiative heat flux in the y-direction	
M	Magnetic Parameter	
R	Radiation parameter	
P_r	Prandtl number	
E_c	Eckert number	
L_e	Lewis Number	
N_b	Brownian motion parameter	
N_t	Thermophoresis parameter	

8. Mailing Address:

Professor Dr. Md. Mahmud Alam.
Mathematics Discipline,
Khulna University, Khulna-9208, Bangladesh
E-mail: *alam_mahmud2000@yahoo.com*
** E-mail: *ferdowsmohammad@yahoo.com*